PHYSICAL REVIEW B VOLUME 23, NUMBER 6 15 MARCH 1981

Surface electronic structure of calcium, strontium, and barium

L. Ley, G. P. Kerker, and N. Mårtensson*
Max-Planck-Institut für Festkörperforschung, 7 Stuttgart 80, Federal Republic of Germany
(Received 13 August 1980)

The density of surface states in Ca, Sr, and Ba is determined by x-ray-induced photoemission. Surface-related peaks at 0.6 and 1.6 eV (Ca), 0.5 and 1.4 eV (Sr), and 0.35 and 1.0 eV (Ba) below the Fermi level E_F are identified. The bandwidth in Ca and Ba narrows by ~20% at the surface. Self-consistent pseudopotential calculations for a seven-layer slab of Ca (111) and Ca (001) give the surface density of states in good agreement with experiment. The high-lying surface peak at $(E_F - 0.6)$ eV can be identified with a band of surface states which exists both at the (111) and the (001) surface. It has a dangling-bond-like character. The peak at $(E_F - 1.6)$ eV can be identified with a band of surface states which is found at the (001) surface. Its charge density is localized in cavity regions near the surface formed by the first and second atomic layer. Both surface bands are found in energy gaps of the projected bulk band structure.

I. INTRODUCTION

The electronic surface properties of simple metals have attracted relatively little interest compared to those of transition metals and semiconductors. The reasons are primarily that the surface properties of transition metals and their compounds are of greater practical importance in the fields of catalysis and corrosion, whereas the surface properties of semiconductors play an important role in devices which involve contacts and junctions. Moreover, there are experimental advantages in detecting surface states in semiconductors. Those surface states that lie within the fundamental gap can be detected by spectroscopic methods (photoemission, yield spectroscopy, and optical absorption) and they often dominate the electronic transport of free semiconductor surfaces. The surface states of semiconductors have therefore been extensively investigated both experimentally[1] and theoretically.[2] In metals surface states occur in gaps that exist only in certain regions of the Brillouin zone (BZ) and they overlap with bulk states in energy. This makes a distinction between bulk and surface states difficult. Using angular-resolved photoemission from single crystals one can choose emission in those directions of the Brillouin zone where gaps and possible surface states related with these gaps are observed. This technique has so far been applied to a number of transition metals[1] and to Al as the only simple metal.[3] Gartland and Slagsvold[3] identified a surface state on the (100) face of Al and followed its dispersion along $\overline{\Gamma X}$ in the surface Brillouin zone. This surface state is a bona fide surface state up to about the middle of the surface Brillouin zone since it lies in a gap of the projected bulk band structure.[3-5] Beyond that point the gap closes but the surface-sensitive feature in the angle-resolved photoemission spectrum remains. It assumes the character of a surface resonance as surmised by Gartland and Slagsvold[3] and proved by Krakauer *et al.*[6] The intensity of the surface resonance is no less than that of the true surface state.

An experimental situation somewhat between that of a metal and a semiconductor prevails in the divalent metals Ca, Sr, and Ba. The strong hybridization of the s-p band with the d states leads to a "hybridization minimum in the density of states (DOS)" at the bottom and the top of the d bands.[7] The lower of these hybridization minima coincides with a reduction in the free-electron part of the DOS brought about by the touching of the Fermi sphere with the BZ boundary. Both effects add and lead to an extremely low density of states right at the Fermi level E_F in these metals. From the pressure dependence of the resistivity it appears that Ca and Sr might even undergo a transition from a metal to a semimetal between 200 and 300 kbars.[8] The possibility of such a transition for Ca was pointed out by Vasvari *et al.*[9] on the basis of volume-dependent band-structure calculations. It is therefore expected that surface states that might occur in gaps of the projected bulk band structure near E_F are readily detected even in angle-integrated photoemission measurements on polycrystalline samples due to the low overall density of states near the top of the valence bands. That this is indeed the case for Ca, Ba, and Sr is shown in the next section. In Sec. III the first calculation of the electronic surface structure of Ca is presented based on a self-consistent pseudopotential method. The results of this calculation are used in Sec. IV to interpret the origin of surface-related features in the photoemission spectra.

II. EXPERIMENT

A. Method of surface enhancement in photoemission

The surface densities of states, $N_s(E)$, of Ca, Sr, and Ba were derived from the x-ray- (Al $K\alpha$, 1486.6 eV) induced photoelectron spectra (XPS). The information about $N_s(E)$ is contained together with $N_B(E)$, the bulk density of states, in those parts of the photoemission spectrum to which only electrons contribute that have not suffered any energy losses on their way through the sample. The probability to suffer an inelastic collision per unit length of travel is given by $1/\lambda$, where λ is the mean free path of the electrons. If λ is assumed to be a direction-independent property of the material, the average sampling depth d of the photoelectrons is $d = \lambda \sin\theta$. The angle θ is the electron take-off angle measured relative to the surface. By varying θ the sampling depth d is readily changed and in this way the relative contributions of $N_s(E)$ and $N_B(E)$ are varied.[10]

To be specific we take the mean free path of the photoelectrons to be $\lambda = 30$ Å. This value is appropriate for electrons with a kinetic energy of about 1480 eV according to the compilation by Ibach.[11] We shall further assume that the surface density of states is limited to the first 3 Å of the metal. This corresponds to about 1.3 lattice spacings for Ca in the [100] direction. In Fig. 1 we have plotted the surface emission I_s from this layer relative to the total no-loss emission [i.e., $I_s/(I_s+I_B)$] as a function of the electron take-off angle θ. We find that for $60° \leq \theta \leq 90°$ the surface contributes no more than 10% to the total emission, whereas this contribution rises steeply for glancing take-off angles. Between $\theta = 60°$ and 7° the surface contribution to the total spectrum changes by a factor of 7. So far we have not considered the refraction of the electrons as they cross the surface. Since they have to overcome a potential barrier, they will be refracted away from the surface normal and the exit angle will be smaller than the angle with which they approach the surface from inside the solid. The latter angle is the one that determines d and the refraction will therefore reduce the surface enhancement at low take-off angles. The dashed line in Fig. 1 takes the refraction into account assuming a surface barrier of 10 eV and a kinetic energy of the electrons of 1480 eV.

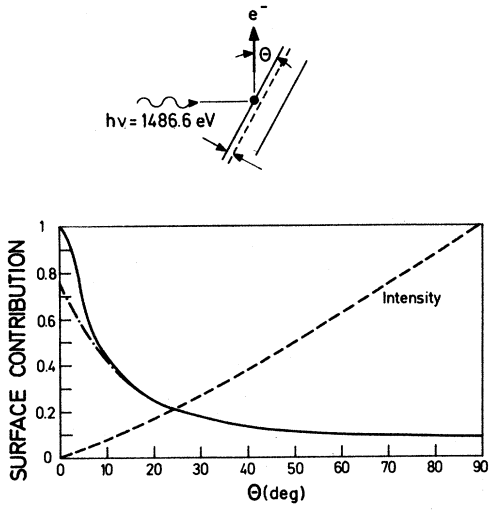

FIG. 1. Ratio of the photoemission intensity from the first 3 Å relative to the total signal strength as a function of electron take-off angle θ.

B. Experimental details

The measurements were performed in a HP-5950 A ESCA spectrometer employing monochromatized Al $K\alpha$ x rays ($h\nu = 1486.6$ eV) as excitation source. A special sample holder was used that allowed rotation of the sample so that the electron exit angle could be changed while the angle between the x-ray beam and the acceptance direction of the electrons remained constant. The electron acceptance cone had an opening angle of about 3°. The resolution of the spectrometer varied between 0.55 eV full width half maximum (FWHM) at $\theta = 7°$ and 0.7 eV at $\theta = 56°$. The samples of Ca, Sr, and Ba were prepared by evaporating thin films *in situ* onto fire-polished glass substrates. The high reactivity of the metals and in particular the high affinity of Ba to N_2 made special precautions necessary to obtain clean films. Vacuum-distilled material was introduced under an argon atmosphere into the spectrometer chamber and the evaporation from well outgassed charges took place in a vacuum below 10^{-10} Torr. In this way films could be obtained which did not show any contamination in the XPS spectrum, even at take-off angles as small as 7°.

C. Results

Figure 2 shows the valence-band spectra of Ca, Sr, and Ba taken at 56° and 7° take-off angle. The spectra have been smoothed and they are broadened by convoluting them with Gaussians to give the same resolution of 0.8 eV for both angles. According to Fig. 1 the 56° spectra are representative of the bulk with only 6% surface contribution. The 7° spectra contain approximately equal amounts of surface and bulk emission. The bulk contribution to the 7° spectra has been subtracted using an appropriately scaled 56°

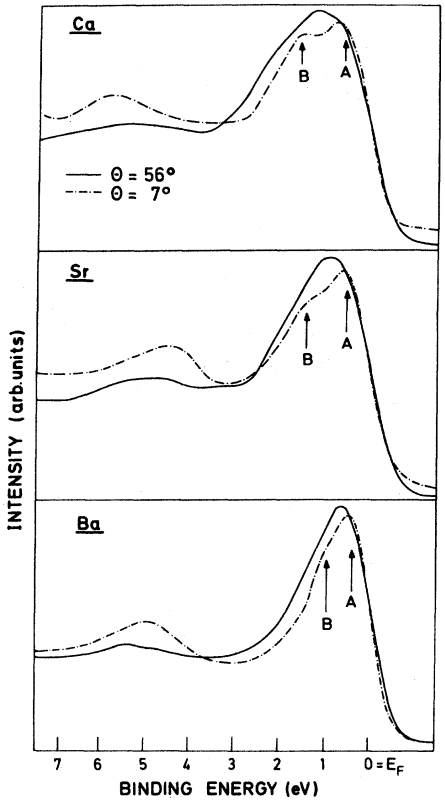

FIG. 2. XPS valence-band spectra of Ca, Sr, and Ba taken at two take-off angles.

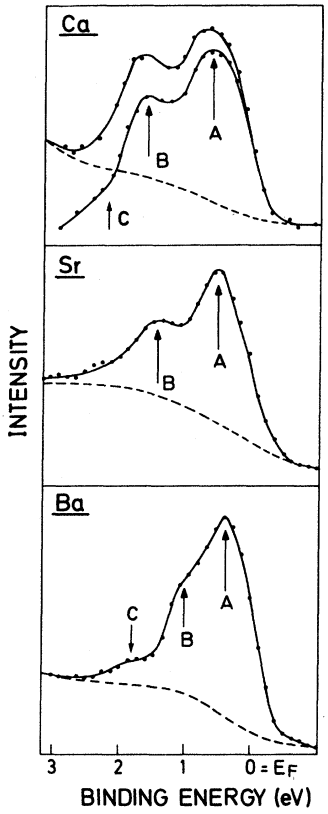

FIG. 3. Experimental surface density of states obtained from spectra taken at $\theta = 7°$ after correction for bulk contribution.

spectrum in each case. The result is shown in Fig. 3 for all three metals. The valence-band emission extends from the Fermi energy E_F, to about 3-eV binding energy. It is superimposed on a background of inelastically scattered electrons. An estimate of this background is shown by the dashed lines in Fig. 3. At higher binding energies this background shows considerable structure due to plasmon excitations. In the 7° spectra a first intense plasmon loss shows up at 4.7 eV (Ca), 3.6 eV (Sr), and 4.2 eV (Ba) below the valence-band maximum (see Fig. 2). These and further losses are observed on all core levels as well and they are discussed elsewhere.[12] In the 56° spectra these losses are reduced in intensity and therefore assigned to surface plasmons. A broadening of the plasmons is also observed with an indication of two maxima in Sr and Ba. The loss at higher binding energy is likely due to bulk plasmons. The bulk valence-electron distributions (VED's) are essentially one-peaked structures with a width that decreases monotonically from 3.6 eV in Ca to 2.2 eV in Ba (see also Table I). Some fine structure can be distinguished on the Ca and Sr spectra taken at 56° before they are broadened.

Turning now to the surface VED's we observe a drastic change. Instead of the one-peaked structure of the bulk VED's, two peaks emerge that are labeled A and B in Figs. 2 and 3. These two peaks bracket the maximum of the bulk VED: The more prominent peak A at the low-binding-energy side close to E_F and peak B at the high-binding-energy side. There is a systematic movement of both peaks towards E_F from Ca to Sr and the peak separation decreases with decreasing bulk bandwidth in the same order.

Features A and B are clearly established even before the 7° spectra have been corrected for the bulk contribution. A less pronounced "foot" (labeled C in Fig. 3) can be identified in addition after the correction has been performed. The energies of all characteristic features are listed in Table I.

It is already evident from the raw data of Fig. 2 that the width of the 7° spectra is reduced from that of the bulk VED's. The full widths at half maximum (FWHM) of the bulk and surface VED's are listed in Table I. For Ca and Ba the reduction at the surface is 20%. In the case of Sr both

TABLE I. Characteristic energies of the bulk and surface valence-band spectra of calcium, strontium, and barium. Energies are given in eV, binding energies refer to the Fermi level, and uncertainties in the last digits are given in parentheses.

	Ca		Sr		Ba	
	Bulk	Surface	Bulk	Surface	Bulk	Surface
Total width	3.6(2)	3.0(2)	2.8(2)	2.6(2)	2.2(3)	2.2(2)
Full width at half maximum	2.8(1)	2.4(1)	2.3(1)	2.3(1)	1.8(2)	1.5(2)
Features in surface spectra A		0.6(1)		0.5(1)		0.35(05)
Features in surface spectra B		1.6(1)		1.4(1)		1.0(1)
Features in surface spectra C		2.4(1)		2.3(1)		1.8(1)
Separation $B-A$		1.0(1)		0.9(1)		0.65(10)
Plasmon energy	4.0(2)	4.7(2)	4.0(2)	3.6(2)	4.4(2)	4.4(2)

spectra have about the same width at half maximum.

III. THEORETICAL CALCULATIONS

A. Method

We employ a self-consistent pseudopotential method which is very similar to the method used by Cohen and co-workers in calculating the surface electronic structure of semiconductors.[13] The calculation was done for both Ca(001) and Ca(111). The surface of the semi-infinite crystal is simulated by either of the two surfaces of a seven-layer material slab. In addition to the periodicity in the plane of the slab, we introduce an artificial periodicity in the perpendicular direction by repeating the slab indefinitely with an empty space separation equivalent to five material layers. We will show below that this choice is sufficient to detect the most prominent surface features.

We construct an effective one-electron pseudo-Hamiltonian for the valence-band electrons which has the form

$$H = p^2/2m + V_{ps} + V_{Coul} + V_{xc} . \quad (1)$$

V_{ps} is taken to be a superposition of Ca^{2+} ionic pseudopotentials

$$V_{ps}(\vec{r}) = \sum_{\vec{R}} V_{ps}^{ion}(\vec{r} - \vec{R}) . \quad (2)$$

Using a method described in Ref. 14, $V_{ps}^{ion}(\vec{r})$ is generated from an *ab initio* calculation for a free Ca atom in the configuration $4s^{0.8}\,4p^{0.7}\,3d^{0.5}$ to obtain a s, p, and d angular-momentum component. Self-consistent bulk linearized augmented plane-wave (LAPW) calculations indicate that this configuration is very likely to correspond to bulk calcium.[15] The resulting nonlocal core pseudopotential has a soft core, it yields normalized pseudo-wave-functions which are smooth and nodeless inside the core region and converge identically to the atomic valence wave functions outside the core. The core pseudopotential is energy independent over an energy interval of 2 a.u. around the atomic levels; that is, even though it is constructed from a given atomic configuration it reproduces the atomic valence levels of different configurations within 0.002 a.u. in the given energy interval.

The ionic pseudopotential is screened by a Coulomb potential V_{Coul} which is obtained from the (pseudo) valence charge density $\rho(\vec{r})$ using

$$\nabla^2 V_{Coul}(\vec{r}) = -8\pi\rho(\vec{r})$$

and by a local exchange-correlation V_{xc} for which we have taken the expression given by Hedin and Lundqvist.[16] The Schrödinger equation for the Hamiltonian Eq. (1) is solved iteratively in reciprocal space for the superlattice until input and output screening potential are equal within 0.002 a.u. Using a very efficient interation scheme[17] this accuracy was achieved within nine iteration steps starting with a potential constructed from overlapping atomic charge densities. Approximately 20 plane waves per atom were used to describe accurately both the occupied sp part and the mainly empty d part of the valence bands. This corresponds to an energy cutoff of 1.8 Ry. Additional 300 plane waves up to a cutoff of 4 Ry were included via Löwdin's perturbation scheme[18] to obtain eigenlevels accurate within less than 0.1 eV. The screening potential during iteration is obtained both for Ca(111) and Ca(001) from the charge density based on a uniform mesh of 15 $\vec{k}_{\parallel}$ points in the irreducible part of the two-dimensional Brillouin zone. The stability of the final self-consistent screening potential is checked by increasing the number of $\vec{k}_{\parallel}$ points in the mesh.

B. Results

It is well known[5] that true surface states occur in absolute gaps and in symmetry gaps of the projected bulk band structure. The identification of surface states or resonances is therefore greatly facilitated by projecting the bulk energy bands against the two-dimensional Brillouin zone. In Fig. 4 the projected bulk band structure is shown for the (111) face of Ca along the three principal symmetry lines of the surface Brillouin zone which is added as an inset. The surface bands which are found from our slab calculation are indicated by dashed lines. Vertical cross-hatching denotes the continuum of bulk states. The most prominent band of surface states below the Fermi level, labeled by A, occurs in a rather large energy gap around $\bar{\Gamma}$ which shows up as two gaps along the lines from $\bar{\Gamma}$ to $\bar{M}$ and from $\bar{\Gamma}$ to $\bar{K}$. Such a gap is already anticipated from the bulk band structure[7,19] along the Σ line. The surface band is slightly split off from the lower bulk band spectrum with an upward dispersion. It can be traced up to the Fermi level where it starts to merge into the bulk spectrum. Additional surface bands occur in energy gaps of the unoccupied part of the projected band structure at $\bar{M}$ and $\bar{K}$. Their extent in the surface Brillouin zone is, however, much smaller than the extent of the occupied surface band A. Since it is the aim of the calculation to correlate possible surface states with photoemission spectra we will not further investigate unoccupied surface states.

The situation at the (001) face is similar. Again, from the bulk band structure along the Δ line one expects a gap at $\bar{\Gamma}$, the center of the surface Brillouin zone. This gap should be more shifted towards the Fermi level compared to the gap at the (111) face. This is indeed what we find by projecting the bulk energy bands against the two-dimensional Brillouin zone of the (001) surface. The result is shown in Fig. 5 along the three principal symmetry lines of the surface Brillouin zone. As before, crosshatching is used for the bulk continuum, vertical and horizontal crosshatching refers to states of different symmetry, and dashed lines are bands of true surface states. An absolute energy gap extends from $\bar{\Gamma}$ along $\bar{\Sigma}$, and along $\bar{\Delta}$ and $\bar{Y}$. Along $\bar{\Sigma}$ near the $\bar{M}$ point the absolute gap becomes a symmetry gap, because bulk states of Σ_2 symmetry are allowed. There are two distinct surface bands which exist in the gap regions. The one labeled A along $\bar{\Delta}$ and $\bar{\Sigma}$ has the same origin as the surface band A at the (111) surface as we will see later on. It is, however, much closer to the Fermi level than its counterpart at the (111) surface. The second surface band labeled B starts at $\bar{X}$ and exists along the $\bar{Y}$ line with upward dispersion. It can be easily traced almost up to $\bar{M}$. We note that due to the use of a thin film rather than a semi-infinite crystal, each surface band should be doubly degenerate. However, this degeneracy is usually split, because of mutual interactions between the two slab surfaces. The thinner the film is, the more the degeneracy is split and the more complicated it is to identify surface states. Our surface energy bands given in Figs. 4 and 5 are therefore supposed to be an average of the two bands being even or odd with respect to inversion or reflection in the central layer of the slab. For a seven-layer Ca film one finds that the two bands are usually split by 0.4 eV.

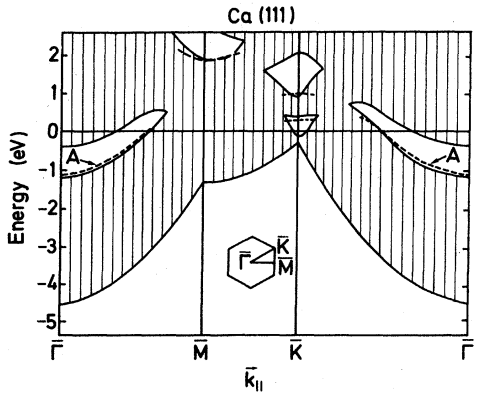

FIG. 4. Projected bulk band structure of the (111) face of Ca along the three principal symmetry lines of the surface Brillouin zone together with the bands of surface states. For further explanation see text. All energies are quoted with respect to the Fermi level.

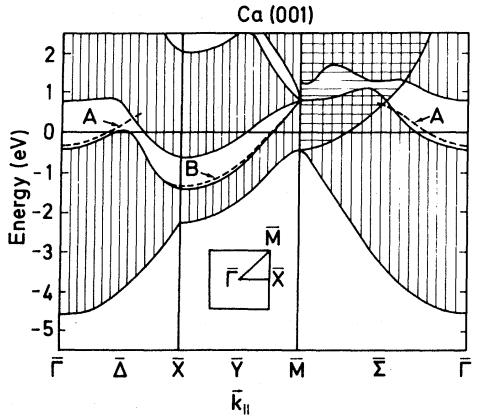

FIG. 5. Projected bulk band structure of the (001) face of Ca along the three principal symmetry lines of the surface Brillouin zone together with the occupied bands of surface states. See text.

The density of states caused by these surface states is presented in Fig. 6 and compared with the bulk density of states for calcium. One peak is obtained for Ca(111) centered at −0.5 eV, whereas a two-peak structure appears for Ca(001) with peaks centered at −0.1 and −1.4 eV. The maximum of the bulk density of states occurs at −1.1 eV.

We can easily obtain information about the origin and the shape of the surface states by using contour plotting of charge densities as a "microscope." Figure 7 shows a contour plot of the total (pseudo) valence charge density near a Ca(001) surface. In the close vicinity of the surface layer the electronic charge density is considerably perturbed compared to the distribution found in the central layer. Charge coming not only from the surface atoms but also from the second-layer atoms is spilled out into the vacuum. However, the "healing effect" is quite strong. Apart from Friedel oscillations the charge density starts to develop its typical bulk distribution already in the second atomic layer. Charge bonds quite similar to those in covalent semiconductors occur along the nearest-neighbor directions. A plateau of a relatively high charge density is found in the center of the interstitial regions. From the total charge-density distribution one can expect two types of surface states at the (001) surface: "Dangling-bond" states which should arise from cutting the bonds between the nearest-neighbor atoms, and "back-bond" states which should arise from perturbing the charge in the interstitial region due to the presence of the surface. In Fig. 8 the charge distribution of the surface band A found at the (001) surface is displayed in a contour plot. This band clearly has dangling-bond character. The maximum of the charge density occurs outside the slab in the vacuum region, the states belonging to this band decay exponentially inside the slab, and the atomic layers are regions of very low density. In contrast to the states of the surface band A, the states of the surface band B are back-bond states. In Fig. 9 a contour plot of a B state at $\bar{X}$ is displayed. Its charge is concentrated in the cavity region formed by the sur-

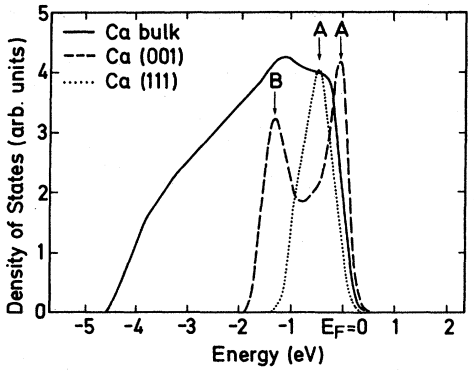

FIG. 6. Density of states of the occupied surface bands of Ca(001) and Ca(111) together with the self-consistent Ca bulk density of states. The labels of the peaks correspond to the labels of the surface bands in Figs. 4 and 5. The original histograms have been broadened by a Gaussian to simulate the experimental resolution.

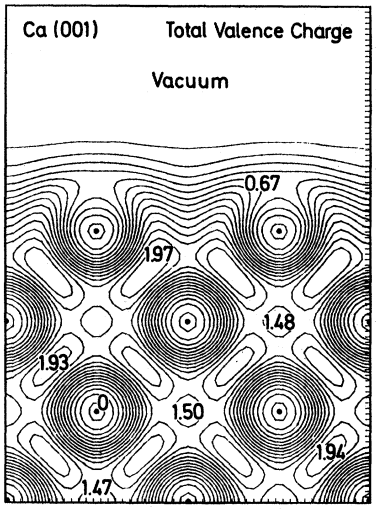

FIG. 7. Contour plot of the total charge density near the (001) surface of Ca. The contour plane is the (110) plane. The density is normalized to unity over the unit cell. The atomic positions are indicated by black dots. The separation of adjacent contour lines is $\frac{1}{15}$ of the maximum density value given in the plot.

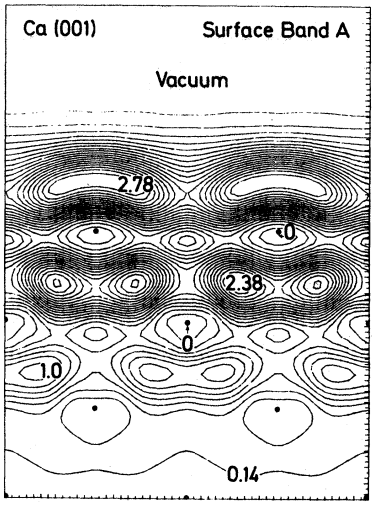

FIG. 8. Contour plot of the charge density of the surface band A at the Ca(001) surface. Contour plane and labels are the same as in Fig. 7.

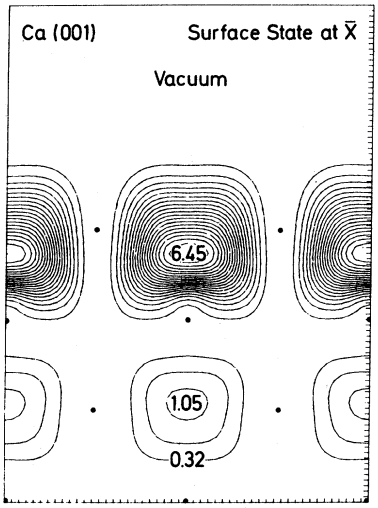

FIG. 9. Contour plot of the charge density of the occupied Ca(001) surface state at the $\bar{X}$ point. Conventions as given in Fig. 7.

face atoms and the atoms in the second layer, a remainder of the bulk interstitial region. Although this state is more pulled towards the slab it decays fairly rapidly and can be easily identified as a surface state in the seven-layer slab.

The occupied surface band A at the Ca(111) surface has dangling-bond character, no back-bond band is found at this surface below the Fermi level. The (111) face is the closed packed face among the low-index faces of the fcc lattice, perturbations of the electronic charge density are more restricted to the (111) surface region than at other surfaces. As a consequence back-bond states do not appear as strong surface states but may exist within the bulk spectrum as weak resonances with a large decay length. It is obvious that such states cannot be detected in thin-film calculations.

IV. DISCUSSION

The results of the theoretical calculation offer a simple explanation of the surface-related features in the photoemission spectra of Ca, Sr, and Ba. If we assume that the contributions of the polycrystalline samples to the surface spectra are dominated by (001) and (111) surfaces, the peak labeled A in Figs. 2 and 3 can be associated with the dangling-bond surface bands at the (001) and (111) surface. In practice, the experimental peaks represent an average of the contributions from all faces present at the surface area of the sample. This might explain that for Ca the upper peak is shifted to higher binding energies by 0.3 eV. The peak labeled B in Figs. 2 and 3 is then primarily caused by the back-bond surface band at the (001) surface. This result can also be stated in a different way: The photoemission spectrum of a clean (111) surface should exhibit only *one* peak near the Fermi level. The presence of the peak B indicates that the samples contained a considerable amount of (001) surface planes. This is a remarkable result because from statistical reasons one would expect that the closed-packed (111) plane dominates the surface spectrum. In Table II the theoretical results for Ca are summarized and compared with the experimental data. Apart from the two-peak structure which characterizes the surface the calculation provides some indication that there exists a back-bond resonance both at the (001) and (111) surface which starts at −3.6 eV at $\bar{\Gamma}$ with a strong upward dispersion. Its contribution to the density of states would produce a broad but weak peak around −2.5 eV for Ca. We did not include this resonance band in Figs. 4 and 5 because a seven-layer slab is not thick enough to uniquely identify such states as surface resonances.

From the knowledge of the Fermi level E_F the work function can be evaluated as the difference between the potential far outside in the vacuum and E_F. The value for the vacuum potential in our calculation is assumed to be negligibly different from the value of the potential at the midpoint of the vacuum region between adjoining slabs. The calculated values for Ca are also given in Table II and are compared with the experimental value for the polycrystalline sample.[20] Taking into account the artificial geometry imposed by the supercell technique the agreement can be considered to be reasonable. The calculated value for Ca(001) is practically equal to the experimental work function. The calculated work function for Ca(111) is smaller than the values obtained from jellium-model calculations by 0.1–0.4 eV.[21]

We finally note that the calculated Ca bulk bandwidth is about 1 eV larger than the experimental

TABLE II. Some characteristic electronic bulk and surface data for Ca. Energies are given in eV and are quoted with respect to the Fermi level.

Calcium	Experiment	Theory (111)	Theory (001)
Surface peak A	−0.6 ± 0.1	−0.5	−0.1
Surface peak B	−1.6 ± 0.1		−1.4
Surface peak C	−2.4 ± 0.1	−2.5	−2.5
Work function	2.87 ± 0.06[a]	3.4	2.9
Total bulk bandwidth	3.6 ± 0.2	4.5	

[a] From Ref. 20.

value. The tendency of getting too large a bandwidth in all band-structure calculations for Ca (Ref. 7) could be related to the fact that many-particle excitation effects are not included in our ground-state method. Inclusion of these effects can reduce the bandwidth as has been shown recently for diamond.[22]

V. SUMMARY

The surface electronic structure of calcium, strontium, and barium has been determined by surface-enhanced x-ray photoemission. The surface spectrum of all three elements exhibits a characteristic two-peak structure which bracket the maximum of the bulk density of states. Moving from Ca to Sr the two-peak structure is shifted towards the Fermi level and the peak separation becomes smaller with decreasing bulk bandwidth. The results of a self-consistent pseudopotential calculation for a seven-layer Ca(111) and Ca(001) film indicate that the upper peak is associated with dangling-bond-like surface states which exist both at the (111) and the (001) surface. The lower peak can only be identified with surface states at the (001) surface which are localized in cavity regions near the surface formed by the first and second atomic layers.

ACKNOWLEDGMENT

We thank H. T. Künzel for his advice on the sample preparation, W. Neu and G. Krutina for their technical help, and Dr. O. K. Andersen and Dr. O. Gunnarsson for their interest and helpful comments.

---

*Permanent address: University of Uppsala, S-75121 Uppsala, Sweden.

[1]See, e.g., *Photoemission and the Electronic Properties of Surfaces*, edited by B. Feuerbacher, B. Fitton, and R. F. Willis (Wiley, Chichester, 1978).

[2]See, e.g., J. A. Appelbaum and D. R. Hamann, Rev. Mod. Phys. 48, 479 (1976).

[3]P. O. Gartland and B. J. Slagsvold, Solid State Commun. 25, 489 (1978).

[4]D. S. Boudreaux, Surf. Sci. 28, 344 (1971).

[5]E. Caruthers, L. Kleinman, and G. P. Alldredge, Phys. Rev. B 8, 4570 (1973); 9, 3325 (1974).

[6]H. Krakauer, M. Posternak, and A. J. Freeman, Phys. Rev. Lett. 41, 1072 (1978).

[7]J. W. McCaffrey, J. R. Anderson, and D. A. Papaconstantopoulos, Phys. Rev. B 7, 674 (1973).

[8]H. G. Drickamer and C. W. Frank, *Electronic Transitions and the High Pressure Chemistry of Solids* (Chapman and Hall, London, 1973), p. 117–119.

[9]B. Vasvari, A. O. E. Animalu, and V. Heine, Phys. Rev. 154, 535 (1967).

[10]C. S. Fadley, Faraday Discuss. Chem. Soc. 60, 18 (1975).

[11]H. Ibach, in *Electron Spectroscopy for Surface Analysis*, edited by H. Ibach (Springer, Berlin, 1977), p. 1.

[12]L. Ley, N. Mårtensson, and J. Azoulay, Phys. Rev. Lett. 45, 1516 (1980).

[13]See, for example, M. Schlüter, J. R. Chelikowsky, S. G. Louie, and M. L. Cohen, Phys. Rev. B 12, 4200 (1975).

[14]G. P. Kerker, J. Phys. C 13, L189 (1980).

[15]H. L. Skriver, private communication.

[16]L. Hedin and B. I. Lundqvist, J. Phys. C 4, 2064 (1971).

[17]G. P. Kerker, unpublished.

[18]Löwdin's perturbation scheme is described in detail by M. L. Cohen and V. Heine in *Solid State Physics*, edited by H. Ehrenreich, F. Seitz, and D. Turnbull (Academic, New York, 1970), Vol. 24, p. 37.

[19]V. L. Moruzzi, J. F. Janak, A. R. Williams, in *Calculated Electronic Properties of Metals* (Pergamon, New York, 1978).

[20]L. Gaudart and R. Rivoira, Appl. Opt. 10, 2336 (1971).

[21]V. Sahni and J. Gruenebaum, Phys. Rev. B 19, 1840 (1979).

[22]G. Strinati, H. J. Mattausch, and W. Hanke, Phys. Rev Rev. Lett. 45, 290 (1980).